

Controlling the shell microstructure in a low-temperature-grown SiNWs and correlating it to the performance of the SiNWs-based micro-supercapacitor

Ankur Soam¹ · Nitin Arya¹ · Alka Kumbhar¹ · Rajiv Dusane¹

Received: 16 January 2016 / Accepted: 5 May 2016 / Published online: 18 May 2016
© The Author(s) 2016. This article is published with open access at Springerlink.com

Abstract We report here the effect of a controlled modification of the shell microstructure around the crystalline core of a silicon nanowire (SiNW) grown at a low (320 °C) temperature by the hot wire chemical vapor processing (HWCVP) method. We demonstrate these effects through the evaluation of the performance of a micro-supercapacitor (μ -SC) device fabricated with these SiNWs having different shell structures. It is to be emphasized that the shell microstructure could be modified through a controlled interplay of the process parameters during the growth. A careful optimization of the shell microstructure in these nanowires during its low-temperature deposition has led to a μ -SC with capacitance value of 94 $\mu\text{F}/\text{cm}^2$. This result opens up exciting opportunities for HWCVP-grown SiNWs to be employed for on-chip μ -SC and other low-temperature applications.

Keywords Hot wire chemical vapor deposition · Low temperature · Silicon nanowires · Micro-supercapacitor · Microstructure · Nanocrystalline

Introduction

Integration of on-chip energy sources has drawn much attention in recent years as per the demands of miniaturization (Shen et al. 2013; Beidaghi and Gogotsi 2014;

Ferris et al. 2015; Zhang et al. 2005). Microbattery has already been incorporated in on-chip applications (Zhang et al. 2005). However, complex structures and other drawbacks with the batteries have motivated researchers to look for alternate energy storage devices (Xia et al. 2012). In this regard, μ -SC may be used as a replacement, or in conjunction with the battery. μ -SCs are easy to fabricate, environment friendly and have a long life with high power densities (Cotz and Carlen 2000). Many carbon-based materials have been proposed for μ -SC applications (Lufrano and Staiti 2010; Obreja 2008; Kalugin et al. 2008; Yoo et al. 2011; Korenblit et al. 2010). However, the incompatibility of their fabrication process with the standard Si chip technology hampers their integration into MEMS. Therefore an electrode material is required which is compatible and scalable enough to meet MEMS requirements. In this context, SiNWs having the required properties and the compatibility with MEMS could be promising as electrode material for μ -SC applications. Moreover, their properties such as length, diameter and doping level can be predictably altered to control the capacitance of SiNW-based μ -SC (Schmidt et al. 2009).

Till date, some amount of work has already been done on SiNWs-based μ -SC. Choi et al. (Choi et al. 2010) have demonstrated the use of the porous SiNWs in supercapacitor. Later on, Thissandier and co-workers (Thissandier et al. 2012, 2013a, b, 2014; Berton et al. 2014) also did an extensive study on SiNWs, used as electrodes in μ -SC. However, this study involved a high processing temperature (600 °C) for SiNWs which limited their use in low-temperature applications such as flexible devices and on-chip μ -SC. To resolve this issue, a few attempts have been made for the fabrication of SiNWs directly on a silicon wafer by wet chemical etching processes (Alper et al. 2012; Chatterjee et al. 2014). However, with this approach,

✉ Rajiv Dusane
rodusane@iitb.ac.in

Ankur Soam
ankursoam007@gmail.com

¹ Semiconductor Thin Films and Plasma Processing Laboratory, Department of Metallurgical Engineering and Materials Science, Indian Institute of Technology Bombay, Mumbai 400076, India

it is very difficult to fabricate a μ -SC with two-electrode geometry on a single Si substrate. Moreover, low throughput, requirement of chemicals and its applicability to a particular substrate (Si) cripple the effectiveness of this approach. In contrast, cost-effective and well-defined SiNWs synthesized at low temperatures by the HWCVP technique via the VLS mechanism have tremendous potential in resolving these issues and show promise for their prospective use in low-temperature applications.

In this work, SiNWs are synthesized by the HWCVP technique via the VLS mechanism, which enables the growth at a substrate temperature of 320 °C using Sn as catalyst. This low-temperature process opens up the possibility for the direct fabrication of μ -SC on flexible substrates (Nathan et al. 2012). These SiNWs are found to have a core-shell structure (Adachi et al. 2010). The effect of the structural properties of the shell on the capacitance value has been studied for first time in this paper. After the growth of SiNWs, their capacitor performance was evaluated by cyclic voltammetry (CV) and galvanostatic charge/discharge methods in an ionic electrolyte.

Experimental details

SiNWs were grown on stainless steel (SS 316) substrate with dimensions of $1.5 \times 1.5 \text{ cm}^2$ by the HWCVP technique via the vapor-liquid-solid (VLS) mechanism using Sn as a catalyst. This substrate also works as a current collector for the electrode of SiNWs. The substrate was sonicated in methanol for 5 min for cleaning. A thin film of Sn was then deposited on it by thermal evaporation of Sn powder. This film was exposed to atomic hydrogen, generated by a heated tantalum filament in the HWCVP chamber which resulted in Sn nanotemplate (Meshram et al. 2013). Using this nanotemplate, synthesis of SiNWs was done by passing SiH_4 gas over the heated filament at 1700 °C. Scanning electron microscopy (SEM), transmission electron microscopy (TEM) and Raman spectroscopy were employed to gather information on the morphology (length and diameter), microstructure and bonding configuration of SiNWs. Thereafter, μ -SC was fabricated comprising two identical electrodes of SiNWs separated by a filter paper dipped in an ionic electrolyte (trifluoromethylsulfonamide). This assembly was then mounted on a Teflon holder for electrochemical measurements.

Results and discussion

In Fig. 1a, the SEM image depicts the morphology of sample 1 of the as-grown SiNWs. The image shows that the HWCVP-grown SiNWs are dense, which is required for the

superior performance of the μ -SC. The diameter, measured at the center of the wires, of the as-grown SiNWs is found to be in the range of 250–300 nm as shown in Fig. 1b. Figure 1c is the TEM image of a single SiNW, which shows a spherical particle of Sn on the top of the SiNW, confirming the growth via VLS mechanism (Wagner and Ellis 1964). The SiNW is tapered toward the top and it can also be seen from Fig. 2 that the nanowire has a core-shell structure. Detailed information on the core-shell structure and tapering of SiNWs can be found in the literature (Adachi et al. 2013; Misra et al. 2013; Rathi et al. 2011). It is clear from Fig. 2 that the core and the shell of the SiNWs are made up of single-crystalline and hydrogenated amorphous Si (a-Si:H), respectively. The crystalline core is the result of the axial growth of Si through the VLS mechanism, while the radial deposition of Si-containing species leads to the formation of the outer shell of varying microstructure and thickness. Thus, the diameter of the SiNWs is always larger than the used nanotemplate size (25–35 nm, Fig. 1d). The thickness of the a-Si:H layer on the crystalline core decreases from bottom to the end of SiNWs (Fig. 2). Raman spectrum in Fig. 1e also shows two peaks at 480 and 520 cm^{-1} , which are attributed to the amorphous shell and crystalline core, respectively.

To study the capacitive behavior of these SiNWs, a CV was performed between voltages 0 and 1.3 V at a scan rate of 40 mV/s, as shown in Fig. 3. The quasi-rectangular shape of the CV curve indicates the near-capacitor characteristics of SiNWs. The maximum voltage limit for the electrolyte used is determined to be 1.3 V. Beyond this limit, the CV shows a Faradaic peak which is the result of decomposition of the electrolyte on the SiNWs surface. The SiNWs capacitance is calculated using the following equation (Alper et al. 2012), $C=2 \cdot I/v \cdot A$, where C is the capacitance per unit area, v is the scan rate, A is the SiNWs electrodes area and $I=(I_+ + I_-)/2$. I_+ and I_- are the currents measured during charging and discharging states, at 0.8 V. The specific capacitance for this structure is calculated to be 62 $\mu\text{F}/\text{cm}^2$. Amorphous Si has an electrical conductivity of $\sim 10^{-10} \text{ S}/\text{cm}$. Since these SiNWs have a core-shell structure, the electrical properties of the shell inherently contribute to the resultant electrical conductivity of SiNWs and thus play a decisive role on the capacitance value for a given crystalline core size (length and diameter). Hence, a large thickness of the shell causes a large potential drop across it owing to its poor electrical conductivity, thereby leading to the low value of the capacitance. Though the surface area is another important factor which affects the capacitance (Thissandier et al. 2014; Alper et al. 2012), the inevitable dependence of capacitance on the shell's structural properties has been put before the geometrical aspects of SiNWs in this study. It can therefore be concluded that SiNWs with an amorphous shell will always result in a lower capacitance value of μ -SC.

Fig. 1 **a** FEG-SEM image of the as-grown SiNWs using the HWCVP technique **b** NWs diameter distribution **c** TEM image of a single SiNW **d** Sn nanotemplate **e** Raman spectrum of the SiNWs

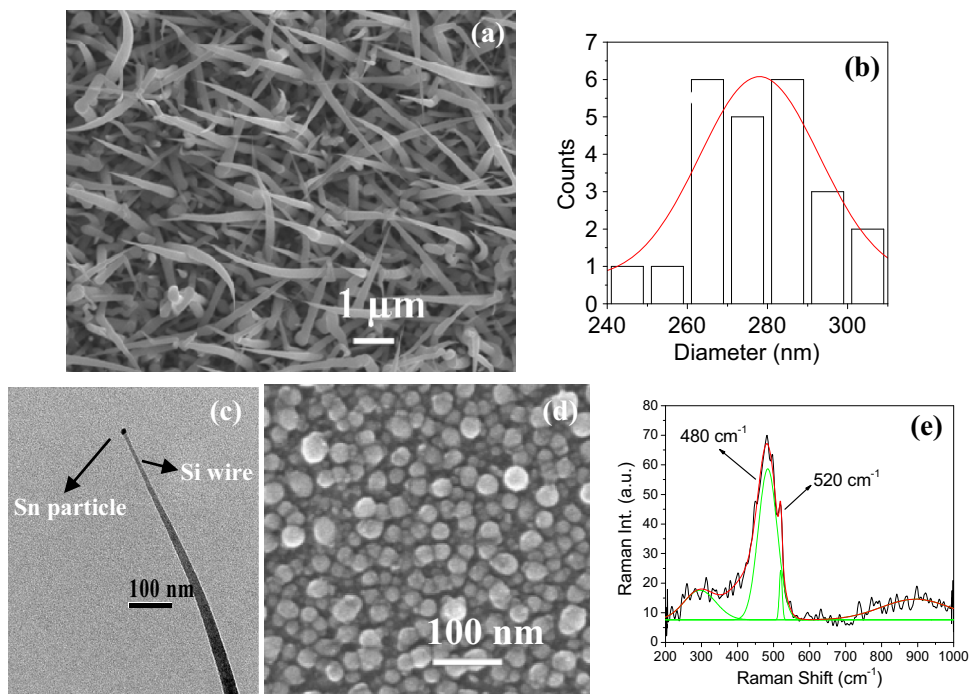
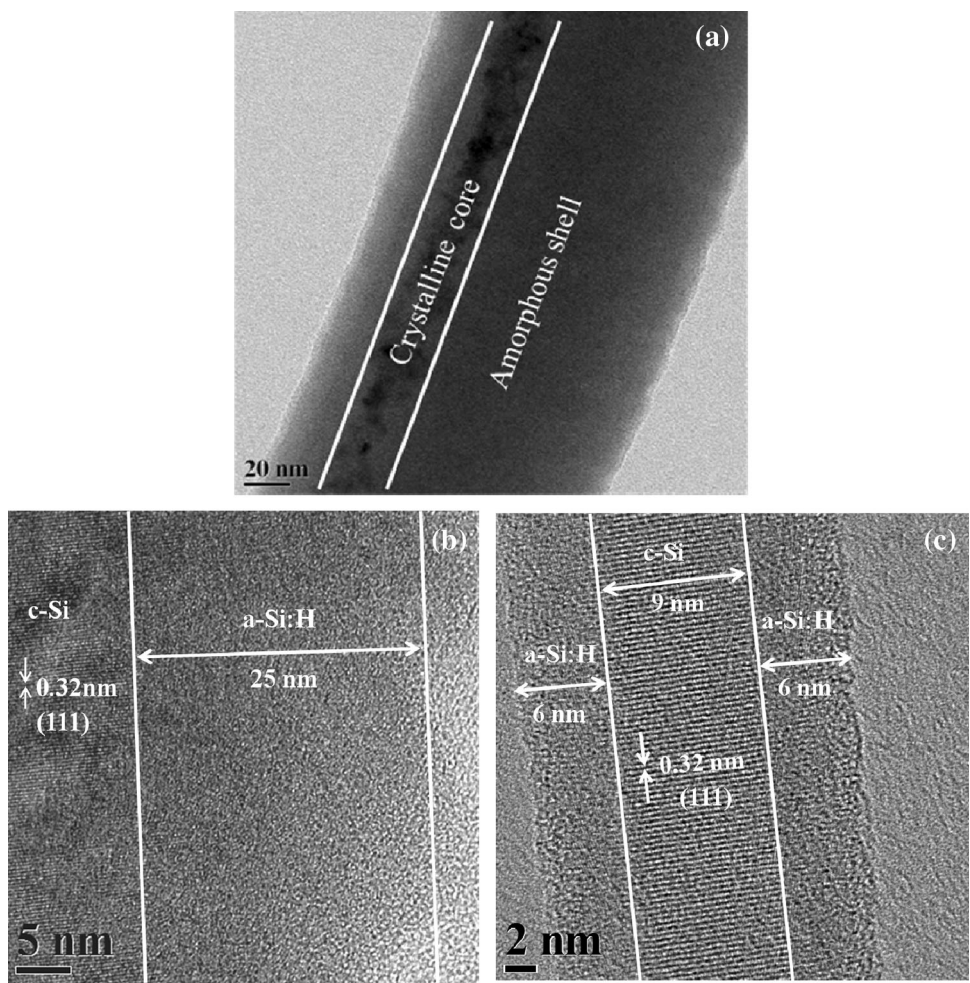


Fig. 2 **a** Bright field HR-TEM image depicting the crystalline core (*darker region*) and amorphous shell (*lighter region*) of an SiNW, **b** taken at the *side* and **c** near the *top*



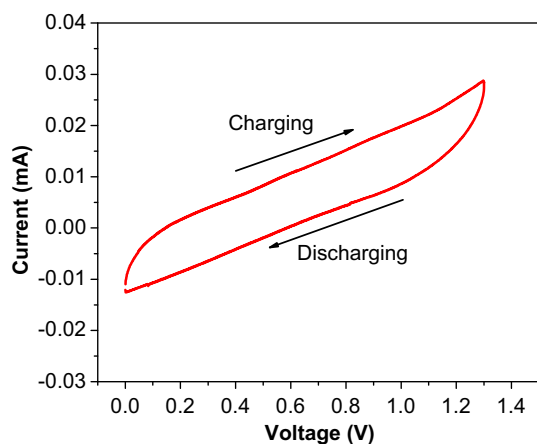


Fig. 3 CV curve of SiNWs which have amorphous shell on the crystalline core

Table 1 HWCVP parameters

Process parameter	a-Si shell	nc-Si shell
Substrate temperature	320 °C	320 °C
Filament temperature	1700 °C	1700 °C
SiH ₄ flow	5	1
Chamber pressure	10 mtorr	30 mtorr
Growth time	30 min	30 min

Thus, proper control of the microstructure and the thickness of the shell are absolutely required to extract superior performance from the capacitor. We now carefully alter the process conditions to prepare sample 2, so that the shell microstructure changes to nanocrystalline (nc-Si:H). This change is brought about by precisely tuning the HWCVP process parameters, viz. the reduction in SiH₄ flow up to 1 sccm and increase in the chamber pressure up to 30 mtorr. Table 1 summarizes the process parameters used for obtaining different shell structures.

The morphology of the as-grown SiNWs with these process conditions is shown in Fig. 4a, which also shows the needle-shaped geometry of sample 2 similar to sample 1. But, the difference in the microstructures can be easily seen while comparing TEM images in Figs. 2a, 5d of a-Si:H and nc-Si:H shell, respectively. SiNWs in sample 1 have smooth surface, whereas SiNWs in sample 2 show nanoflakes type of structure. It can be seen that these SiNWs of sample 2 consist of nc-Si:H shell (electrical conductivity $\sim 10^{-5}$ S/cm) rather than an a-Si:H one (Fig. 5). Additionally, the diameter of the SiNWs is also found to be lesser than earlier as shown in Fig. 4b.

Raman spectrum in Fig. 4c has an additional 506 cm⁻¹ peak which confirms the presence of nanocrystallites (<10 nm) and thus establishes the nanocrystalline nature of the shell (Bibo Li et al. 1999). The change in the shell

structure can be attributed to much lower availability of Si-containing species and the increased hydrogen residence time inside the chamber, which favor the growth of nc-Si:H instead of a-Si:H (Matsuda 1999). These conditions also cause the deposition rate of the overgrowing coating to be lowered, resulting in reduced thickness of the shell. Hence, the diameter of SiNWs calculated now is approximately 140–170 nm as shown in Fig. 4b, which is much lesser than the 250–300 nm previously recorded. The specific capacitance of these SiNWs is calculated to be 94 $\mu\text{F}/\text{cm}^2$ from the CV as depicted in Fig. 6, which shows a considerable increase of almost 50 %.

Raman crystallinity factor (X_c) determined in samples 1 and 2 are 10 and 50 %, respectively (Droz et al. 2004). It can be inferred that the increases in the X_c comes from the nanocrystalline contribution. Hence, these corroborations from the Raman spectra along with HR-TEM results prove that the microstructure of the shell is nanocrystalline rather than amorphous. HR-TEM images also reveal that the shell of sample 2 has nc-Si:H nanocolumns having a shoot-like appearance (Fig. 5). A similar structure of SiNWs consisting of nc-Si:H nanocolumns has also been reported in HWCVP-synthesized SiNWs using indium as catalyst and with a lot of H₂ dilution (Chong et al. 2011). The galvanostatic charging/discharging curves were recorded at a constant current density of 5 $\mu\text{A}/\text{cm}^2$ and presented in Fig. 7. These curves have a triangular shape and the voltage varies linearly with time, confirming the ideal capacitor behavior of SiNWs $\mu\text{-SC}$. The amount of charge stored in the capacitor is proportional to the charging or discharging time. We can see that the SiNWs with nc-Si:H shell take larger time as compared to SiNWs with an a-Si:H one during discharging, which again confirms that the SiNWs with nc-Si:H shell have superior charge-storing capacity. Therefore, it is established that the change of the microstructure from amorphous to nanocrystalline leads to an increase in the resultant electrical conductivity of SiNWs, which manifests itself in the improvement of capacitance value of the $\mu\text{-SC}$ by ~ 50 %. Further improvement in the capacitance value is possible by optimizing other properties of the SiNWs.

Conclusion

Our investigation of SiNWs synthesized at low temperatures by HWCVP for their proposed use in $\mu\text{-SC}$ application has established that the shell's microstructure significantly affects the capacitance. The microstructure in turn can be controlled by careful adjustment of the growth conditions without introducing any additional step which sacrifices the crucial low-temperature aspect of SiNWs synthesis. A $\mu\text{-SC}$ incorporating the SiNWs with nc-Si:H shell was successfully fabricated and showed a capacitance

Fig. 4 **a** SiNWs (sample 2) synthesized by flowing 1 sccm SiH_4 gas at a chamber pressure of 30 mtorr. **b** Distribution of their diameter. **c** Raman spectrum of the SiNWs

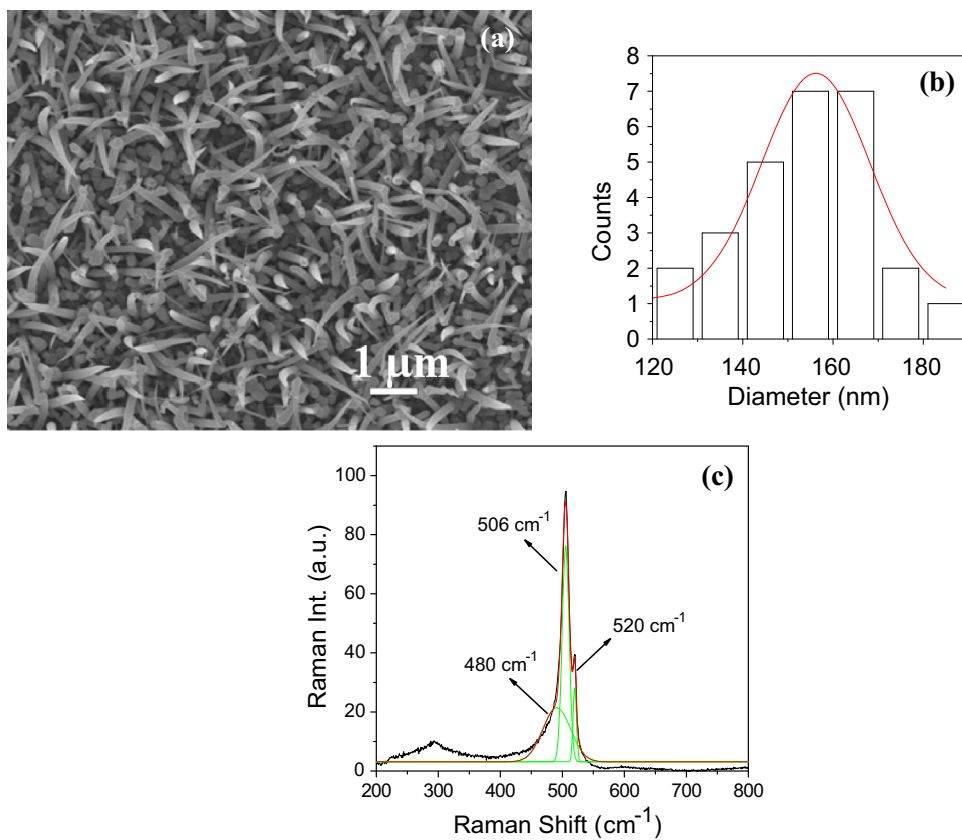
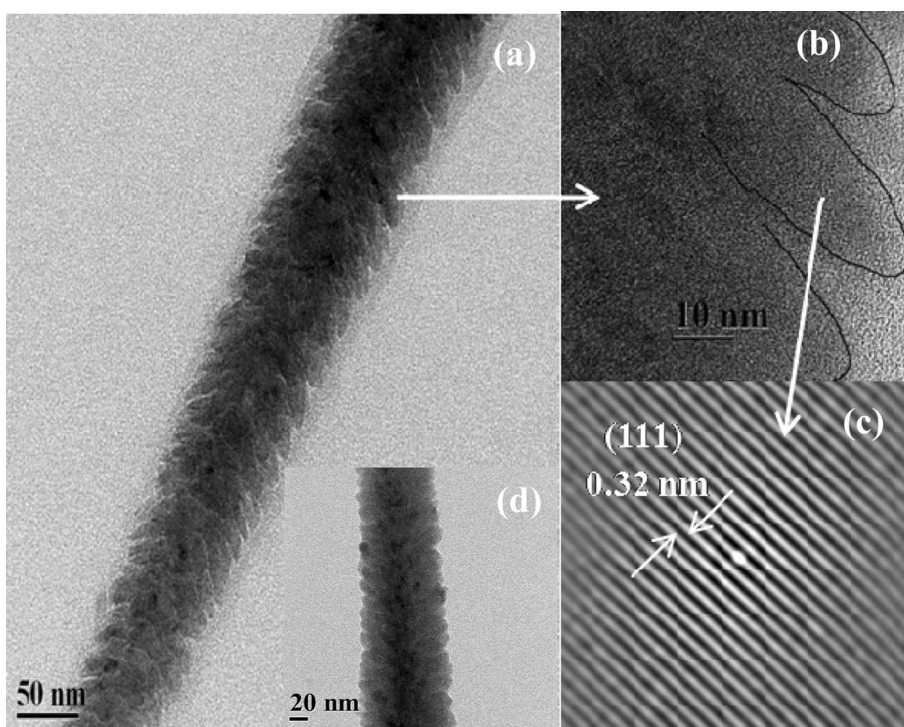


Fig. 5 **a** HR-TEM image taken at a single wire of sample 2 consisting of nanocolumns. **b** HR-TEM image taken at the side of the wire. **c** Crystalline structure of the nanocolumns and **d** TEM image of a different SiNW of sample 2



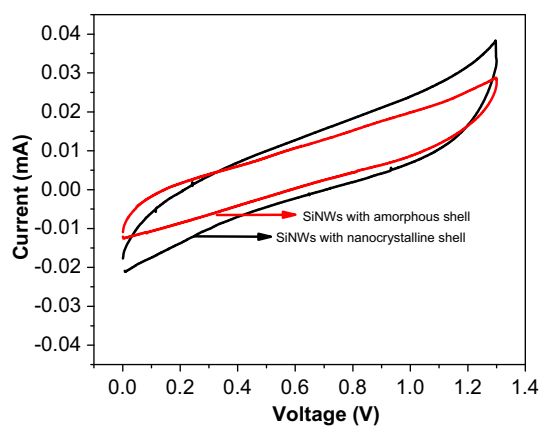


Fig. 6 Comparison of the CV behavior of SiNWs with a-Si:H (red one) and nc-Si:H shell (black one)

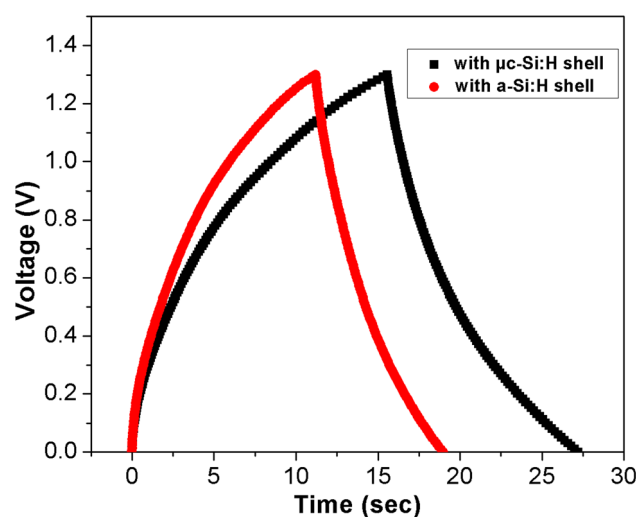


Fig. 7 Galvanostatic charging/discharging curves for sample 1 and sample 2

value of $94 \mu\text{F}/\text{cm}^2$, which is higher than that of SiNWs with a-Si:H shell ($62 \mu\text{F}/\text{cm}^2$). Thus, we have demonstrated a method to increase the capacity of the SiNWs-based μ -SCs fabricated at low temperature.

Acknowledgments Crompton Greaves, Mumbai, is gratefully acknowledged for providing financial support. The authors also thank SAIF, IIT Bombay for providing TEM and SEM facilities. We also thank Prof. V. S. Raja and Prof. S. Parida, Dept. of ME and MS, IIT Bombay, for providing the electrochemical characterization facility. The FIST facility (dual beam FIB, Carl Zeiss microscopy) in ME and MS was also used for this work.

Open Access This article is distributed under the terms of the Creative Commons Attribution 4.0 International License (<http://creativecommons.org/licenses/by/4.0/>), which permits unrestricted use, distribution, and reproduction in any medium, provided you give appropriate credit to the original author(s) and the source, provide a link to the Creative Commons license, and indicate if changes were made.

References

- Adachi MM, Anantram MP, Karim KS (2010) Optical properties of crystalline amorphous core-shell silicon nanowires. *Nano Lett* 10:4093–4098
- Adachi MM, Anantram MP, Karim KS (2013) Core-shell silicon nanowire solar cells. *Sci Rep* 3:1546
- Alper JP, Vincent M, Carraro C, Maboudian R (2012) Silicon carbide coated silicon nanowires as robust electrode material for aqueous micro-supercapacitor. *Appl Phys Lett* 100:163901
- Beidaghi M, Gogotsi Y (2014) Capacitive energy storage in micro-scale devices: recent advances in design and fabrication of microsupercapacitors. *Energy Environ Sci* 7:867–884
- Berton N, Brachet M, Thissandier F, Bideau JL, Gentile P, Bidan G, Brousse T, Sadki S (2014) Wide-voltage-window silicon nanowire electrodes for micro-supercapacitors via electrochemical surface oxidation in ionic liquid electrolyte. *Electrochem Commun* 41:31–34
- Chatterjee S, Carter R, Oakes L, Erwin WR, Bardhan R, Pint CL (2014) Electrochemical and corrosion stability of nanostructured silicon by graphene coatings: toward high power porous silicon supercapacitors. *J Phys Chem C* 118:10893–10902
- Choi JW, Donough JM, Jeong S, Yoo JS, Chan CK, Cui Y (2010) Stepwise nanopore evolution in one-dimensional nanostructures. *Nano Lett* 10:1409–1413
- Chong SK, Goh BT, Aspanut Z, Muhamad MR, Dee CF, Rahman SA (2011) Radial growth of slanting-columnar nanocrystalline Si on Si nanowires. *Chem Phys Lett* 515:68–71
- Cotz R, Carlen M (2000) Principles and applications of electrochemical capacitors. *Electrochim Acta* 45:2483–2498
- Droz C, Sauvain EV, Bailat J, Feitknecht L, Meier J, Shah A (2004) Relationship between Raman crystallinity and open-circuit voltage in microcrystalline Silicon solar cells. *Sol Energy Mater Sol Cells* 81:61–71
- Ferris A, Garbarino S, Guay D, Pech D (2015) 3D RuO_2 Microsupercapacitors with remarkable areal energy. *Adv Mater* 27:6625–6629
- Kalugin ON, Chaban VV, Loskutov VV, Prezhdo OV (2008) Uniform diffusion of acetonitrile inside carbon nanotubes favors supercapacitor performance. *Nano Lett* 8:2126–2130
- Korenblit Y, Rose M, Kockrick E, Borchardt L, Kvit A, Kaskel S, Yushin G (2010) High-rate electrochemical capacitors based on ordered mesoporous silicon carbide-derived carbon. *ACS Nano* 4:1337–1344
- Li B, Yu D, Zhang SL (1999) Raman spectral study of silicon nanowires. *Phys Rev B* 59:1645–1648
- Lufrano F, Staiti P (2010) Influence of the surface-chemistry of modified mesoporous carbon on the electrochemical behavior of solid-state supercapacitors. *Energy Fuels* 24:3313–3320
- Matsuda A (1999) Growth mechanism of microcrystalline silicon obtained from reactive plasmas. *Thin Solid Films* 337:1–6
- Meshram N, Kumbhar A, Dusane RO (2013) Synthesis of silicon nanowires using tin catalyst by hot wire chemical vapor processing. *Mater Res Bull* 48:2254–2258
- Misra S, Yu L, Chen W, Cabarrocas PRi (2013) Wetting layer: the key player in plasma-assisted silicon nanowire growth mediated by Tin. *J Phys Chem C* 117:17786–17790
- Nathan A et al (2012) Flexible electronics: the next ubiquitous platform. *Proceedings of the IEEE* 100:1486–1517
- Obreja VN (2008) On the performance of supercapacitors with electrodes based on carbon nanotubes and carbon activated material-A review. *Physica E* 40:2596–2605
- Rathi SJ, Jariwala BN, Beach JD, Stradins P, Taylor PC, Weng X, Ke Y, Redwing JM, Agarwal S, Collins RT (2011) Tin-catalyzed

- plasma-assisted growth of silicon nanowires. *J Phys Chem C* 115:3833–3839
- Schmidt V, Wittemann JV, Senz S, Gosele U (2009) Silicon nanowires: a review on aspects of their growth and their electrical properties. *Adv Mater* 21:2681–2702
- Shen C, Wang X, Li S, Wang JG, Zhang W, Kang F (2013) A high-energy-density micro supercapacitor of asymmetric MnO₂-carbon configuration by using micro-fabrication technologies. *J Power Sources* 234:302–309
- Thissandier F, Comte AL, Crosnier O, Gentile P, Bidan G, Hadji E, Brousse T, Sadki S (2012) Highly doped silicon nanowires based electrodes for micro electrochemical capacitor applications. *Electrochem Commun* 25:109–111
- Thissandier F, Pauc N, Brousse T, Gentile P, Sadki S (2013a) Micro-ultracapacitors with highly doped silicon nanowires electrodes. *Nanoscale Res Lett* 8:1–5
- Thissandier F, Gentile P, Pauc N, Hadji E, Comte AL, Crosnier O, Bidan G, Sadki S, Brousse T (2013b) Highly N-doped silicon nanowires as a possible alternative to carbon for on-chip electrochemical capacitors. *Electrochemistry* 10:777–782
- Thissandier F, Gentile P, Pauc N, Brousse T, Bidan G, Sadki S (2014) Tuning silicon nanowires doping level and morphology for highly efficient micro-supercapacitors. *Nano Energy* 5:20–27
- Wagner RS, Ellis WC (1964) Vapor-liquid-solid mechanism of single crystal growth. *Appl Phys Lett* 4:89–90
- Xia YY, Jun WL, Guo GY (2012) Silicon-based nanomaterials for lithium-ion batteries. *Chin Sci Bull* 57:4104–4110
- Yoo JJ, Balakrishnan K, Huang J, Meunier V, Sumpter BG, Srivastava A, Conway M, Reddy LM, Yu J, Vajtai R, Ajayan PM (2011) Ultrathin planar graphene supercapacitors. *Nano Lett* 11:1423–1427
- Zhang Z, Dewan C, Kothari S, Mitra S, Teeters D (2005) Carbon nanotube synthesis, characteristics, and microbattery applications. *Mater Sci Eng B* 116:363–368